Aberystwyth University

Empirical assessment of beta dose heterogeneity in sediments
Smedley, R. K.; Duller, G. A.T.; Rufer, D.; Utley, J. E.P.

Research paper

Empirical assessment of beta dose heterogeneity in sediments: Implications for luminescence dating

R.K. Smedley [a,b,*], G.A.T. Duller [b], D. Rufer [c], J.E.P. Utley [a]

[a] School of Environmental Sciences, University of Liverpool, Liverpool, UK
[b] Department of Geography and Earth Sciences, Aberystwyth University, Ceredigion, UK
[c] Institute of Geological Sciences, Universität Bern, Switzerland

ABSTRACT

Optically stimulated luminescence (OSL) dating of single grains is often required to determine an accurate age for partially-bleached sediment by identifying those grains with OSL signals that were well bleached prior to burial. However, single-grain D_e distributions are typically characterised by greater amounts of scatter in comparison to multiple grains. Here we investigate the scatter in single-grain D_e distributions of quartz from 56 proglacial samples associated with the retreat of the last British-Irish Ice Sheet. Our findings provide the first empirical dataset showing that beta-dose heterogeneity can impact the extrinsic scatter in single-grain D_e distributions, in addition to partial bleaching in nature. The additional scatter in single-grain D_e distributions caused by beta-dose heterogeneity suggests that it is inappropriate to apply a fixed threshold to determine between well-bleached and partially-bleached D_e distributions, but the skewness of the D_e distributions could alternatively be used. Auto-radiography and QEMSCAN analyses show that there was a negative relationship between the relative standard deviation (RSD) of the beta-dose heterogeneity and the beta dose-rate. This relationship offers the opportunity to infer the RSD of the beta-dose heterogeneity for each sample using just the beta dose-rate, instead of acquiring empirical data for every sample. For this large suite of sedimentary samples, we observe a minimum OD of 20% arising from the effects of beta-dose heterogeneity (Fig. 3e), which should be added (in quadrature) to the intrinsic OD to determine σ_b for the minimum age model (MAM) to calculate accurate OSL ages and prevent underestimation of the burial age.

1. Introduction

Optically stimulated luminescence (OSL) dating is a geochronological technique that determines the time elapsed since a mineral grain (typically quartz or K-feldspar) was last exposed to sunlight and buried. It can determine ages for sediment deposited in an environment where the OSL signals of all grains were equally reset upon exposure to sunlight (i.e. a well-bleached sediment), in addition to sediments where only a portion of the OSL signals of grains were reset prior to burial (i.e. partially-bleached sediment). In partially-bleached settings, the accuracy of an OSL age is dependent upon the identification of those grains that were well bleached prior to burial, and so the analysis of single grains is typically required to identify these grains (e.g. Duller, 2008). Overdispersion (OD) in single-grain D_e distributions determined from sediment bleached in nature, subsequently buried and not subject to post-depositional mixing, is a combination of intrinsic sources

(luminescence characteristics, instrument reproducibility) and extrinsic sources (external microdosimetry and the extent of bleaching in nature). In glacial settings, it has been common to consider that the scatter caused by the extent of bleaching in nature dominates single-grain D_e distributions due to the limited opportunities for sunlight exposure, usually because grains were transported and deposited by turbulent, sediment-laden water columns. However, it is likely that part of this scatter may have arisen from the effects of microdosimetry (Nathan et al., 2003; Mayya et al., 2006; Rufer and Preusser, 2009; Guérin et al., 2015; Martin et al., 2015; Jankowski and Jacobs, 2018), but no studies have yet obtained the empirical data needed to explore this.

The environmental dose-rate to each grain per annum is a combination of internal and external sources of alpha and beta particles, and external gamma and cosmic rays. Environmental dose-rates are routinely determined from bulk samples taken from the sediment and the material is powdered prior to measurements to homogenise it. In

---

contrast, D_e values are determined from individual quartz grains from a sub-sample of the bulk material. Thus, the bulk estimation of the environmental dose-rate cannot quantify or account for any microscale heterogeneity in the environmental dose-rate to individual grains throughout burial. This microscale heterogeneity of the dose-rate is often referred to as microdosimetry. Etching to remove the surface of the quartz grains by hydrofluoric acid during sample preparation removes the alpha-influenced outer portion of the grain, while the effective ranges of gamma and cosmic rays extend far beyond the volume of a typical OSL sample taken in the field or an individual quartz grain (~200 μm in diameter). Moreover, studies have shown that the internal alpha and beta dose-rates arising from U and Th inclusions within a quartz grain are negligible (e.g. Jacobs et al., 2006). Thus, it is only the external beta dose-rate arising from either K, Rb, U and Th that causes microscale heterogeneities in the dose-rate, where beta particles are deposited as a non-linear function of distance from the point source (e.g. a K-feldspar or zircon grain). Many studies have suggested that the uneven distribution of K within the sediment matrix can cause heterogeneities in the beta dose-rate and result in scatter in D_e distributions (Nathan et al., 2003; Mayya et al., 2006; Guérin et al., 2015; Jankowski and Jacobs, 2018). Guérin et al. (2015) report on how the extrinsic scatter arising from microdosimetry is also a function of grain size and the proportion that the beta dose-rate makes up of the total dose-rate. Recent advances in model simulations of dose-rate (e.g. Guérin et al., 2015; Martin et al., 2015) are continuing to improve our understanding of beta dose heterogeneity and broadly suggest that microdosimetry can account for ~15% overdispersion in a single-grain D_e distribution for a well-sorted sand (Guérin et al., 2015). However, these studies have focussed on a few samples from an area of uniform bedrock and depositional contexts (well-bleached, well-sorted sands) and we lack studies on samples from a variety of different bedrock sources and contexts. Obtaining empirical data from a variety of samples is needed to evaluate the numerical modelling and improve our understanding of this key uncertainty in luminescence dating.

Here we investigate the factors controlling scatter in single-grain D_e distributions determined for quartz from 56 sediment samples deposited by the last British-Irish Ice Sheet. The large suite of sediments used were sourced from variable bedrock types and deposited in different depositional settings (e.g. proglacial lakes, glaciofluvial streams, outwash plains) and so provides an unrivalled opportunity to assess the sources of scatter in single-grain D_e distributions. We report new insights into the extent of extrinsic scatter arising from microdosimetry on single-grain D_e distributions of quartz, which show for the first time that the scatter in a partially-bleached D_e distribution is not solely dominated by the extent of bleaching prior to burial. Our findings have implications for the accuracy and precision of OSL ages when applying age models in all depositional settings.

2. Sedimentary samples

The British-Irish Ice Sheet covered much of northern Britain and Ireland during the Last Glacial Maximum, accumulating ice in the mountains of England, Ireland, Scotland and Wales, with the maximum limit extending as far south as the Isles of Scilly, SW Britain, ca. 26–25 ka (Smedley et al., 2017b). The bedrock geology of Britain and Ireland underlying the former ice sheet is highly variable due the complex geological history of the land masses. Fifty-six samples taken from proglacial sediments in Britain and Ireland were used here, and included
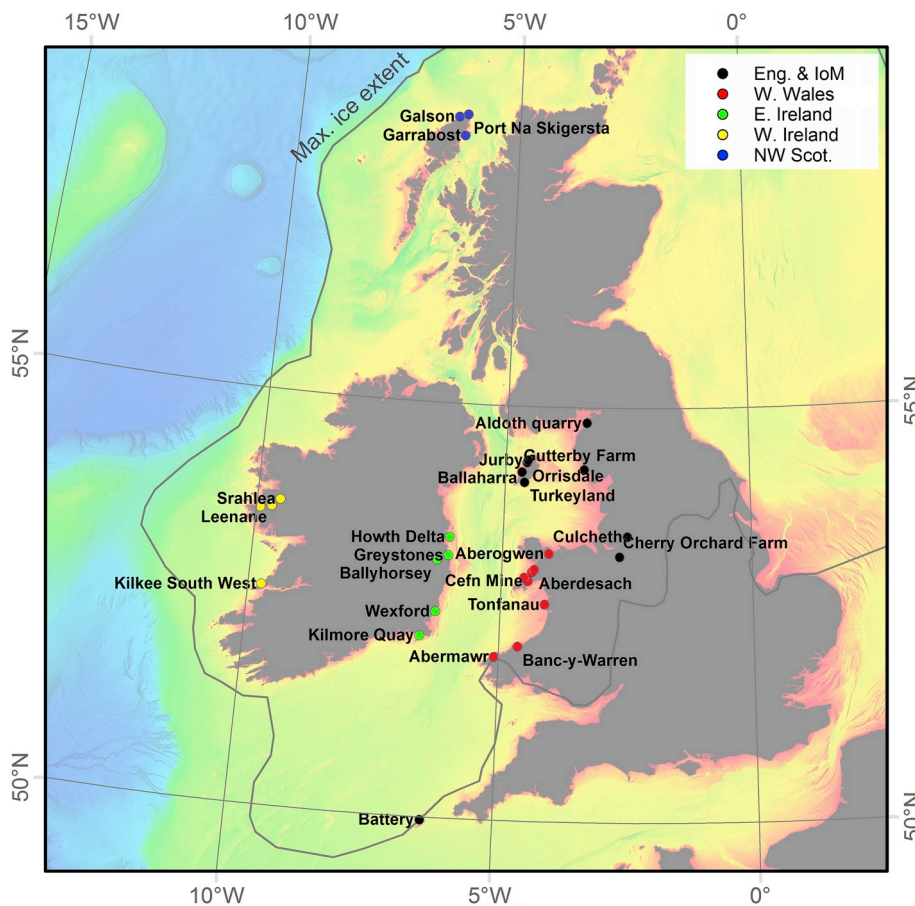

Fig. 1. Locations of the sites sampled for OSL dating in Britain and Ireland plotted over the European Marine Observation and Data Network (EMODnet, http://www.emodnet.eu) topographical data. Also shown is the proposed maximum extent of the British-Irish Ice Sheet. Samples are grouped according to region as shown in Fig. 2.

samples from England and Isle of Man, W Wales, E Ireland, W Ireland and NW Scotland (Fig. 1). The sampling strategy targeted sediments with lithofacies that were likely to have been exposed to sunlight prior to burial (after Thrasher et al., 2009). Five different lithofacies were sampled implying that the sediments were deposited in variable glacial outwash depositional settings; this included sands that were planar (Sp), rippled (Sr), massive (Sm) and horizontally bedded (Sh), and laminated fine-grain sediment (Fl). The samples were not subject to post-depositional mixing (e.g. bioturbation, slumping and remobilisation) as the sedimentary structures were well preserved, however, two exceptions to this are discussed below. The former ice masses that transported and deposited the quartz grains used for OSL dating sourced and mixed materials from lithologically highly variable near- and far-field bedrock (see Table S1 for details on each sample).

3. Experimental details

3.1. OSL dating

Samples were collected in opaque tubes (2 mm thick plastic rim) that were hammered into the sedimentary section to prevent exposure to sunlight during sampling. External beta dose-rates were determined from U, Th, K and Rb concentrations from milled and homogenised bulk sediment samples using inductively coupled plasma mass spectrometry (ICP-MS) and atomic emission spectroscopy (ICP-AES). The beta dose-rates were calculated using the conversion factors of Guérin et al. (2011) and beta dose-rate attenuation factors of Guérin et al. (2012). External gamma dose-rates were determined using in-situ gamma spectrometry. Water contents were estimated considering the field and saturated water contents, and the environmental history for each sample. Cosmic dose-rates were calculated after Prescott and Hutton (1994). The environmental dose-rates for the samples varied from 0.6 to 3.0 Gy/ka (see Table S1 for full details).

All samples were prepared under subdued red lighting conditions in the laboratory. The sedimentary samples were first treated with a 10% v/v dilution of 37% HCl and with 20% of H_2O_2 to remove carbonates and organics, respectively. Dry sieving isolated the coarse grains (ranging from 180 to 250 μm depending upon the sample) and density-separation using sodium polytungstate provided the 2.62–2.70 g cm^{-3} (quartz-dominated) fractions. The quartz grains were etched in 40% hydrofluoric (HF) acid for 1 h to remove contaminating feldspar grains and the outer portion of the quartz grains which was affected by alpha irradiation. After the etching, the quartz grains were washed in 10% HCl to remove any fluorides that may have been produced during HF etching. Grains were mounted into 10×10 grids of 300 μm diameter holes in a 9.8 mm diameter aluminium single-grain disc for analysis.

All luminescence measurements were performed using a Risø TL/OSL DA-15 automated single-grain system (Bøtter-Jensen et al., 2003) equipped with a $^{90}Sr/^{90}Y$ beta source. Stimulation was performed using a green laser (532 nm) and detected through a 2.5 mm thick U-340 filter and convex quartz lens placed in front of the photomultiplier tube. The signal was recorded for a total of 1 s at 125 °C. The OSL signal was summed over the first 0.1 s of stimulation and the background calculated from the final 0.2 s. The instrument reproducibility of the single-grain measurement system was determined to be 2.5%, similar to Thomsen et al. (2005), and was incorporated into the calculation of the D_e uncertainty, in addition to the uncertainty arising from the non-poisson distributions of count rates (after Adamiec et al., 2012, Eq. 10 of Bluszcz et al., 2015). A single aliquot regenerative dose (SAR) protocol was used for OSL analysis (Murray and Wintle, 2000). Preheat plateau tests suggested that the D_e values were independent of preheat temperatures from 160 to 300 °C, but lower preheat temperatures of 180–220 °C for 10 s were used as recuperation was >5% of the response from the largest regenerative dose (~150 Gy) at higher preheat temperatures. A cutheat of 160 °C was used prior to the measurement of the test-dose. Dose-recovery experiments were performed on single grains

taken from every sedimentary unit sampled to determine the amount of scatter in the D_e distributions caused by intrinsic sources (instrument reproducibility, intrinsic luminescence characteristics). The grains were first bleached in the single-grain disc using blue (470 nm) LEDs and given a beta dose between 20 and 57 Gy. All samples recovered the given dose within uncertainties of ±10% and suggested the SAR protocol was appropriate for OSL analyses.

Screening tests were applied to the resulting data throughout the analyses, where grains were only accepted if: (1) the response to the test dose was greater than three sigma above the background; (2) the test dose uncertainty was less than 20%; (3) recuperation was less than 5% of the response from the largest regenerative dose (150 Gy); (4) the recycling ratio was within the range of ratios 0.8 to 1.2; (5) the OSL-IR depletion ratio (Duller, 2003) was within the range of ratios 0.8 to 1.2; (6) the dose-response curve grew monotonically; (7) L_n/T_n could be interpolated on to the dose-response curve to determine a D_e value (i.e. grains with luminescence signals in laboratory saturation where a D_e value could not be determined); (8) the single-grain D_e values were not part of a population of very low doses that were identified by the finite mixture model (FMM) to be inconsistent with the geological context of the sample (e.g. Smedley et al., 2017a,b); only 0–5.5% of the total grains analysed were rejected by Criterion 8. The percentage of grains passing screening criteria and therefore used to determine a D_e for each sample ranged from 0.4 to 8.1% of the total grains analysed. Examples of dose-response curves are shown in Fig. S1.

3.2. Autoradiography

To assess the heterogeneity in the external beta dose, the untreated bulk sediment of 28 out of the 56 samples were analysed using imaging plates (BAS-MS IP, Fuji Photo Film Co.) to produce autoradiographs of the distribution of beta radiation within the sediment matrix. For analysis, unconsolidated sediment samples were sprinkled on to an imaging plate as a 3 mm thick layer and analysed following the methods of Rufer and Preusser (2009). The imaging plates were read out using a BAS-1800 Analyser System (Fujifilm Life Science Co.) and the greyscale image produced for each autoradiograph was a raster of pixels relating to the intensity of beta particle emission at a colour depth of 16 bits per pixel (bpp). Each imaging plate was read out three times and the resulting images were stacked to improve signal/noise ratios (total exposure time ranged from 111 to 183 h). To assess the variability in the beta dose-rate to an individual mineral grain, the data were aggregated so that each pixel was 200 μm by 200 μm. To account for differences in background signals and exposure times between analysis runs, the average background signal was subtracted from each pixel and then normalised to an exposure time of 1 h. This caused the autoradiograph scales to appear to be void of absolute zero; however, this is simply a result of the way the data have been background-corrected and normalised. The relative standard deviation (RSD) of these rasters of beta dose intensity for a 12 cm by 12 cm layer of sediment was calculated to quantify the beta-dose heterogeneity. Sample T4WEXF03 was mounted and exposed to two imaging plates to create two independently determined greyscale images; the results suggested that the high RSD for the greyscale images were reproducible between runs (RSD = 1.13 and 1.27).

3.3. QEM-SCAN

Quantitative evaluation of minerals by scanning electron microscopy (QEMSCAN) is a rapid, repeatable, automated mineralogical analysis technique; it is often referred to as automated scanning electron microscope energy-dispersive X-ray spectroscopy (SEM-EDS). QEMSCAN was used here to provide spatially-resolved mineralogy based on the elemental chemistry of individual grains measured across the surface of polished thin sections, which were made from loose sediment samples poured into a mould and impregnated. QEMSCAN has successfully been

used to provide mineral identification of grains used for luminescence dating in previous studies (e.g. Meyer et al., 2013; Haberlah et al., 2010). Data were acquired with an FEI WellSite QEMSCAN, with a tungsten-filament and operating at 15 kV, equipped with two Bruker EDS detectors. The spacing between measurements, area to scan, and colour used to represent each mineral are all user-defined. QEMSCAN images were acquired for seven out of the 28 samples subject to auto-radiography to assess the proportion of different minerals in the sediment, principally quartz, K-feldspar and sheet silicates (e.g. illite and mica). The QEMSCAN images covered an area of ~16.5 by 16.5 mm.

4. Intrinsic scatter

4.1. Signal intensity

Cumulative light sum plots (Fig. S2) suggest that 90% of the OSL signal was emitted from the brightest 4–41% of single grains in each sample. To assess the absolute brightness of each sample, the total OSL signal emitted by each individual grain in response to a fixed test-dose was normalised to 1 Gy, summed together and then divided by the number of grains analysed (referred to as the normalised OSL signal-intensity for each sample). The range was from 1 to 13 cts/0.1 s/Gy/grain, with a mean (±one standard deviation) of 5 ± 3 cts/0.1 s/Gy/grain. The normalised OSL signal-intensity for each sample has been plotted against the percentage of the brightest grains emitting 90% of

the OSL signal (Fig. 2a). Fig. 2a shows that for samples with a normalised OSL signal ≥6 cts/0.1 s/Gy/grain, ≤ 8% of the brightest grains emitted 90% of the OSL signal. This only included samples from E Ireland, W Wales and England (specifically the Isles of Scilly). For these samples, it is likely that if these grains were mounted on to a multi-grain aliquot, the OSL signal would be dominated by a few brighter grains. The OSL signal for the remaining samples from England and the Isle of Man, W Wales, E Ireland, W Ireland and NW Scotland was not dominated by a few brighter grains (this included samples with a normalised OSL signal < 6 cts/0.1 s/Gy/grain). For these samples, 5–41% of the brightest grains emitted 90% of the OSL signal (Fig. 2a). If quartz grains from these samples were mounted on to a multi-grain aliquot (e.g. small aliquots), the OSL signal would be averaged across multiple grains, which would make OSL dating of partially-bleached sediments more challenging. This supports the findings of Trauerstein et al. (2017) who suggested that signal averaging of single grains can be present even for very dim quartz grains.

4.2. Intrinsic overdispersion

The amount of intrinsic scatter in the D_e distributions from dose-recovery experiments was highly variable between samples, ranging from samples with low OD < 10% (e.g. T4BATT03; Fig. S3h) to higher OD > 30% (e.g. T4BRYN03; Fig. S3r). Previous studies have suggested that variable intrinsic OD values can be determined from dose-recovery
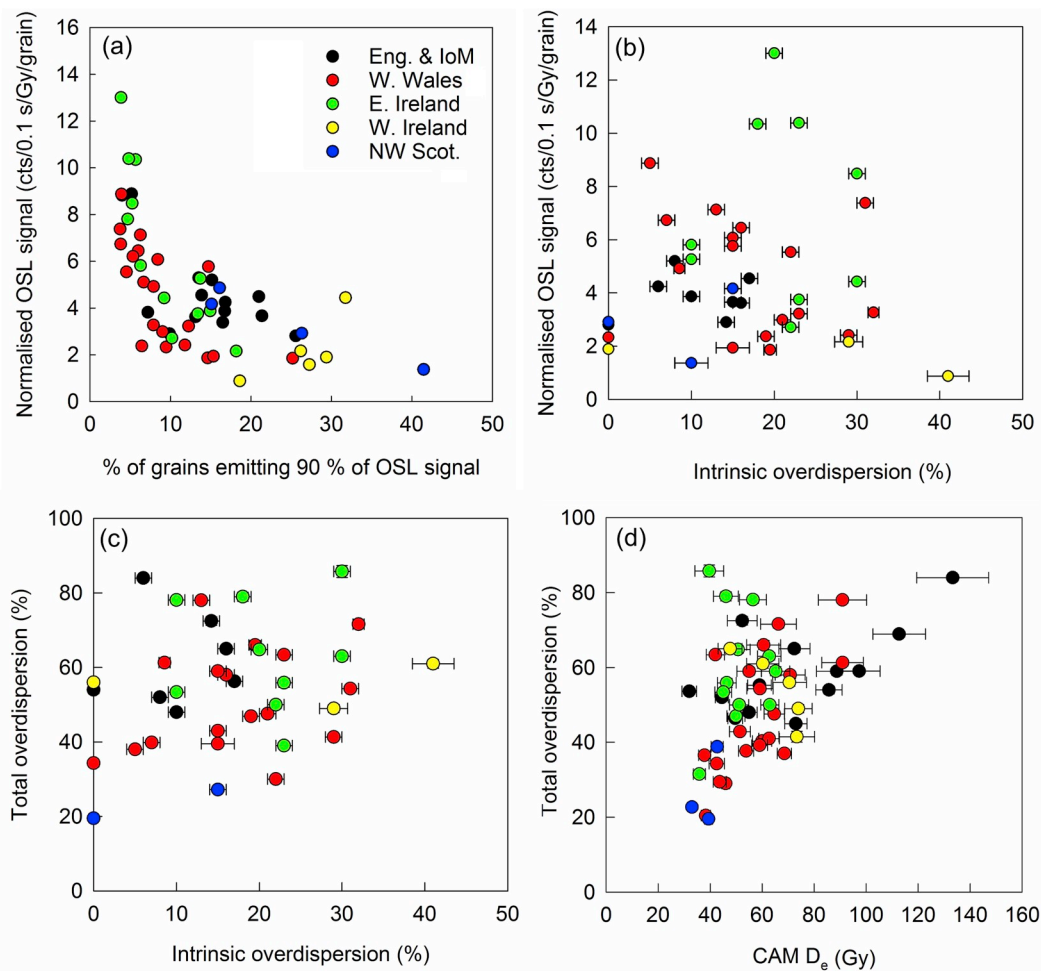

Fig. 2. Percentage of the brightest grains emitting 90% of the OSL signal plotted against the normalised OSL signal-intensity for each sample (a). The intrinsic overdispersion determined from dose-recvoery experiments is plotted against the normalised OSL signal-intensity for each sample (b) and the total overdispersion in the natural burial dose-distributions (c). CAM D_e for each sample plotted against the overdispersion from nature as a percentage (d). Note that samples T4WEXF4B and T8GALS01 are not shown here as they were influenced by post-depositional mixing.

experiments for single grains of quartz, ranging from 2% up to 59% (e.g. Jacobs et al., 2015; Thomsen et al., 2016; Geach et al., 2015). The intrinsic OD determined here for each sample was not dependent upon the normalised OSL signal (Fig. 2b) or the total OD determined from the natural doses (Fig. 2c). Moreover, intrinsic OD values > 25% were determined for samples from a variety of lithofacies (Sr, Sh); thus, it is unlikely that the depositional setting during the last depositional cycle controlled the intrinsic scatter. However, there was a broad regional pattern to the amount of scatter arising from intrinsic sources. The samples from England and Isle of Man and NW Scotland all had OD values of ~10%, while W Wales and E Ireland had values of ~20% and W Ireland had the largest at 30–40%; thus, the variability seen is potentially related to a controlling geographical or geological aspect.
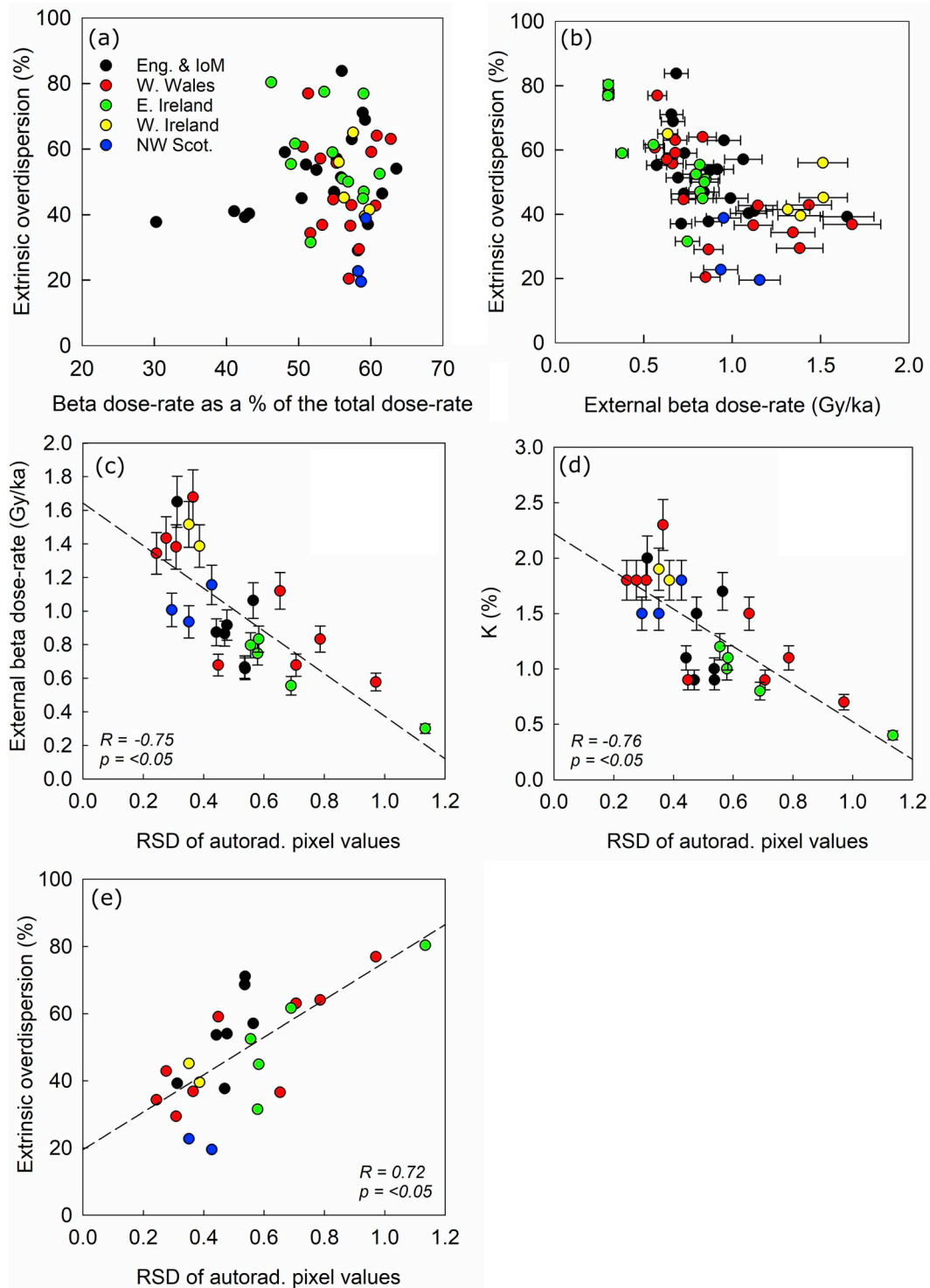

Fig. 3. Comparing the extrinsic overdispersion with the beta dose-rate as a proportion of the total dose-rate (a) and the external beta dose-rate for all samples (b). Relative standard deviation (RSD) of autoradiograph pixel values compared to the external beta dose-rates (c), bulk K concentration (d) and extrinsic overdispersion values (e).

5. Natural dose distributions

OD values determined from burial doses for the 56 samples here ranged from 20 ± 1% (T8SKIG02) to 101 ± 2% (T4WEXF4B) with a mean (±one standard deviation) of 53 ± 15%. This range in OD was reflected in the variability in scatter in the single-grain D_e distributions (see Abanico plots shown in Fig. S4). A proportion of the D_e distributions for samples were symmetrical and had lower OD values than others, which suggested that they were likely well bleached prior to burial while the asymmetric D_e distributions were possibly partially bleached. The central age model (CAM; Galbraith et al., 1999) or average dose model (ADM; Guerin et al., 2017) are routinely used to determine accurate ages for well-bleached D_e distributions, while the minimum age model (MAM; Galbraith and Laslett, 1993; Galbraith et al., 1999) or internal external uncertainty model (IEU; Thomsen et al., 2007) would be applied to partially-bleached D_e distributions. The single-grain D_e distribution of sample T4WEXF4B (Fig. S4ap; OD 101 ± 2%) was different to the other D_e distributions as it contained lower D_e values which suggested that contaminating grains were present in the D_e distribution, likely caused by post-depositional mixing prior to sampling. Also, the sediment sampled for sample T8GALS01 had structures indicative of post-depositional cryoturbation, which was reflected by a population of grains in the D_e distributions measuring lower D_e values (Fig. S4ba). Therefore, samples T4WEXF4B or T8GALS01 were excluded from subsequent analyses here. Fig. 2d shows the D_e value determined using the CAM for each sample plotted against the OD for all samples. As expected, there was no relationship between the CAM D_e value and the OD value.

6. Extrinsic scatter

Extrinsic scatter for a sample that has not experienced post-depositional mixing arises from a combination of partial bleaching (e. g. Olley et al., 1999) and microdosimetry (e.g. Nathan et al., 2003; Mayya et al., 2006; Rufer and Preusser, 2009; Guérin et al., 2015; Martin et al., 2015; Jankowski and Jacobs, 2018). Extrinsic OD can be quantified by subtracting (in quadrature) the OD from intrinsic sources from the total OD in the burial doses. If a sample was well bleached prior to burial, the extrinsic OD should be the result of scatter arising only from external microdosimetry as the scatter arising from the extent of bleaching is negligible. For the samples in this study, there was no relationship between the extrinsic OD and the beta dose-rate as a percentage of the total dose-rate (Fig. 3a). However, when the extrinsic OD was compared to the external beta dose-rate (Fig. 3b), a group of samples had extrinsic OD values that broadly increased with a decreased external beta dose-rate (e.g. the large suite of samples from eastern Ireland; green circles in Fig. 3b). Note that the extrinsic OD shown here also included scatter arising from the effects of partial bleaching, and so any relationship between extrinsic OD and the external beta dose-rate suggests that the influence of microdosimetry on the scatter in a single-grain D_e distribution was significant.

Empirical data were obtained using autoradiography to assess the beta-dose heterogeneity for 28 out of the 56 samples. The autoradiographs varied between samples (e.g. Fig. 4), with images containing different proportions of colder (orange colours in Fig. 4a–d) and hotter (green colours in Fig. 4a–d) spots within the sediment matrix. Visual light images corresponding to each autoradiograph suggested that the hotter spots did not correspond to any distinctive features within the sampled material (e.g. larger grains, regions of thinner or thicker material). The relative standard deviation (RSD) of pixel values was calculated for each image to quantify the variability in the beta dose received by each 200 μm by 200 μm pixel (i.e. grain). RSD values ranged from 0.2 to 1.1. When the RSD of pixel values is compared to the external beta dose-rates (Fig. 3c; $R = -0.75$, $p = < 0.05$), it shows that there was a continuous negative relationship between the two parameters, where the larger RSD were determined for lower beta dose-rates. This suggests that hotspots or coldspots will be present in the sediment matrix for all samples, but that the beta dose-rate will be more heterogeneous for samples with lower dose-rates, which is likely related to the bulk K concentration of the sample (Fig. 3d). This provides empirical data to support the previous studies that have suggested that a dependence of extrinsic scatter on the dose-rate would be related to the beta dose-rate arising from K in the sediment matrix (e.g. Kalchgruber et al., 2003; Rufer and Preusser, 2009; Nathan et al., 2003; Mayya et al., 2006; Cunningham et al., 2012; Guérin et al., 2015). K in the sediment matrix will be located within minerals such as K-feldspar and micas. QEMSCAN was used here to map the distribution of minerals across sub-samples of 16.5 by 16.5 mm of bulk sediment for seven samples, which covered a range of dose-rates and RSD values calculated from the autoradiographs (Fig. 5a; T3COF4, T4ABER01, T4BANC01, T4BATT03, T4BATT06, T4WEXF03, T8SKIG02). The proportions of different minerals were determined from the images (principally quartz, K-feldspar, sheet
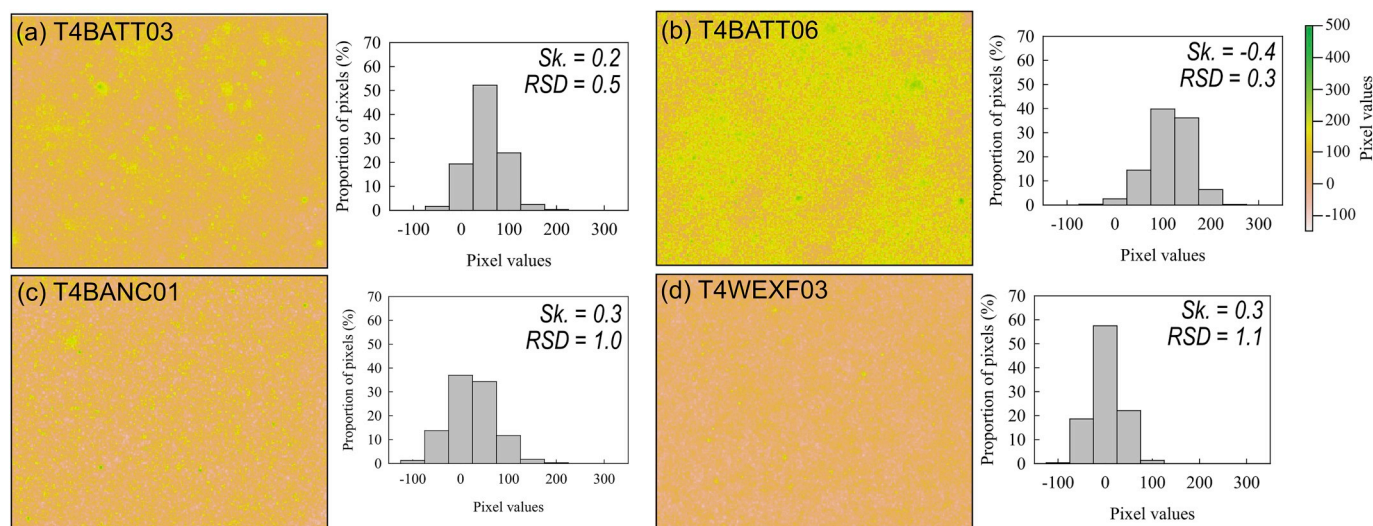

Fig. 4. Examples of autoradiographs showing the beta heterogeneity for samples T4BATT03. T4BATT06, T4BANC01 and T4WEXF03. Each image is corrected for the background signal, normalised to 1 h exposure time and aggregated to 200 μm by 200 μm pixels. Alongside each autoradiograph is the corresponding histogram, relative standard deviation (RSD) and skewness. Note that the autoradiographs for all samples are shown in Fig. S5 and were made from loose sediment samples poured into a mould (i.e. not *in situ* representations).
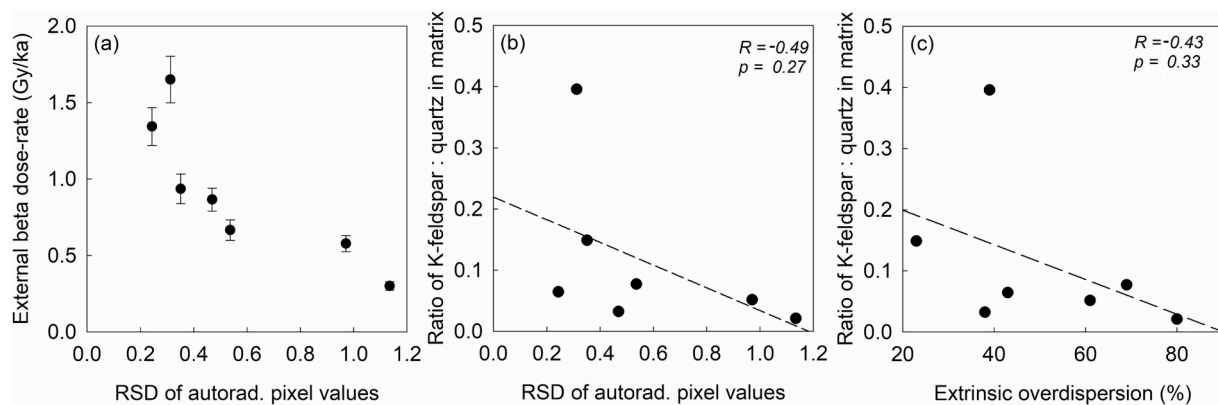
Fig. 5. Relative standard deviation (RSD) of autoradiographs when pixels were aggregated to 200 μm × 200 μm plotted against the external beta dose-rate for the seven samples subject to QEMSCAN® analyses (a) and the proportion of K-feldspar to quartz grains in the matrix (b). Extrinsic overdispersion plotted against the ratio of quartz to K-feldspar in the sediment matrix (c).

silicates and zircon). The QEMSCAN images (Fig. 6) show that the distribution of minerals varies between samples, where the sediment matrix was dominated by quartz (ranging from 50 to 91% of the total) and contained variable amounts of K-feldspar (2–20% of the total), but did not contain any zircon (0–0.03% of the total). Despite the lack of observable accessory minerals such as zircon (which would act as radiation hotspots), some samples featured isolated, large K-feldspar and sheet silicate grains, which would contribute as localised anomalies to the beta radiation field within the sample (e.g. T4BATT06; Fig. 6b).

To assess the relationship between K-feldspar distribution in the sediment matrix and beta-dose heterogeneity, the proportions of K-feldspar to quartz in the sediment matrix (derived from QEM-SCAN) were plotted against the RSD in the beta dose heterogeneity from the autoradiograph for each sample (Fig. 5b). There was a broad negative trend between the two parameters ($R = -0.49$, $p = 0.27$), supporting the interpretation that positively-skewed beta-dose heterogeneity is related to samples with less K-feldspar in the sediment matrix, and vice versa. Moreover, the ratio of K-feldspar to quartz in the matrix was also broadly related to the extrinsic overdispersion (Fig. 5d; $R = 0.43$, $p = 0.33$). This empirical data is consistent with results from numerical modelling simulations which suggested that scatter caused by beta dose heterogeneity was a result of spatial distribution density and location of radionuclide bearing mineral phases such as K-feldspar (e.g. Kalchgruber et al., 2003; Rufer and Preusser, 2009; Nathan et al., 2003; Mayya et al., 2006; Cunningham et al., 2012; Guérin et al., 2015). However, neither of these trends were statistically significant and were likely complicated by the effects of grainsize and sorting in the sediment matrix as suggested by Guerin et al. (2015), in addition to the presence of sheet silicates (e.g. T4BATT06).

7. Implications for luminescence dating

The empirical data from the autoradiography and QEMSCAN (Section 6) show that there was a negative relationship between the RSD of the beta-dose heterogeneity and the beta dose-rate (and K), where the larger RSD values were determined for lower beta dose-rates. Fig. 3e shows that the beta-dose heterogeneity influenced the scatter in the single-grain D_e distributions independently of partial bleaching. Fixed thresholds have previously been adopted to determine between well-bleached and partially-bleached D_e distributions (e.g. 20% overdispersion; Arnold and Roberts, 2009). However, if partial bleaching is not the only factor controlling the shape of the D_e distribution, it will complicate the identification of well-bleached (i.e. apply the CAM or ADM) and partially-bleached (i.e. apply the MAM or IEU model) D_e distributions; thus, it would be inappropriate to apply a fixed threshold to identify well-bleached and partially-bleached D_e distributions. An alternative approach would be to use the symmetry of the D_e

distribution as measured by skewness to assess the extent of bleaching prior to burial, whereby symmetrical D_e distributions were well bleached prior to burial, and partially-beached D_e distributions would be asymmetrical.

The trend between the RSD of the beta-dose heterogeneity and the beta dose-rate (Fig. 3c) offers the opportunity to infer the RSD of the beta-dose heterogeneity for each sample using just the beta dose-rate, instead of performing autoradiography on every sample. The minimum RSD of the beta-dose heterogeneity that was determined was 0.2, which is consistent with the minimum extrinsic OD value that was determined for this dataset of 20% (Fig. 3e). For the CAM or the ADM (Guerin et al., 2017), averaging of the D_e values would overcome these additional sources of scatter. However, an additional 20% OD should be combined (in quadrature) with the intrinsic overdispersion to accurately quantify σ_b for the MAM and prevent age underestimation for this suite of samples. This typically means that age uncertainties will be larger for partially-bleached samples (i.e. MAM) in comparison to well-bleached samples (i.e. CAM). Using glaciofluvial sediments of similar age (~18 ka) from the Llŷn Peninsula as an example (Smedley et al., 2017a), the age uncertainty for the well-bleached sample (T4ABER01) was 9% (1.7 ka), while the partially-bleached sample (T4ADES01) was 17% (3.2 ka).

8. Conclusions

The accuracy and precision of OSL ages is highly dependent upon the application of age models (e.g. CAM and MAM) used to determine an age and so it is important to accurately quantify the different sources of scatter in D_e distributions used for dating. Here we present the first empirical dataset quantifying the scatter caused by beta dose heterogeneity for a large suite of samples from different bedrock sources and depositional bleaching contexts, and show that beta dose heterogeneity is currently an under-declared uncertainty in luminescence dating. We investigated the intrinsic and extrinsic sources of scatter in single-grain D_e distributions of quartz from 56 sedimentary samples from a proglacial environment. Dose-recovery experiments performed on each sample showed that there was large variability between samples (0–41% OD) with broad regional trends suggesting a local bedrock control on intrinsic sources of scatter. When relative standard deviations (RSDs) of the beta-dose heterogeneity were measured using autoradiography and compared to the external beta dose-rate (Fig. 3b), it was observed that there was a negative relationship between the two parameters, independent of partial bleaching. Higher relative standard deviations (RSDs) were linked with lower beta dose-rates due to the presence of hotter spots in a cooler matrix. The additional scatter in D_e distributions caused by beta-dose heterogeneity mean that it would be inappropriate to apply a fixed threshold to determine between well-bleached and partially-bleached D_e distributions, and so the skewness of the D_e distributions
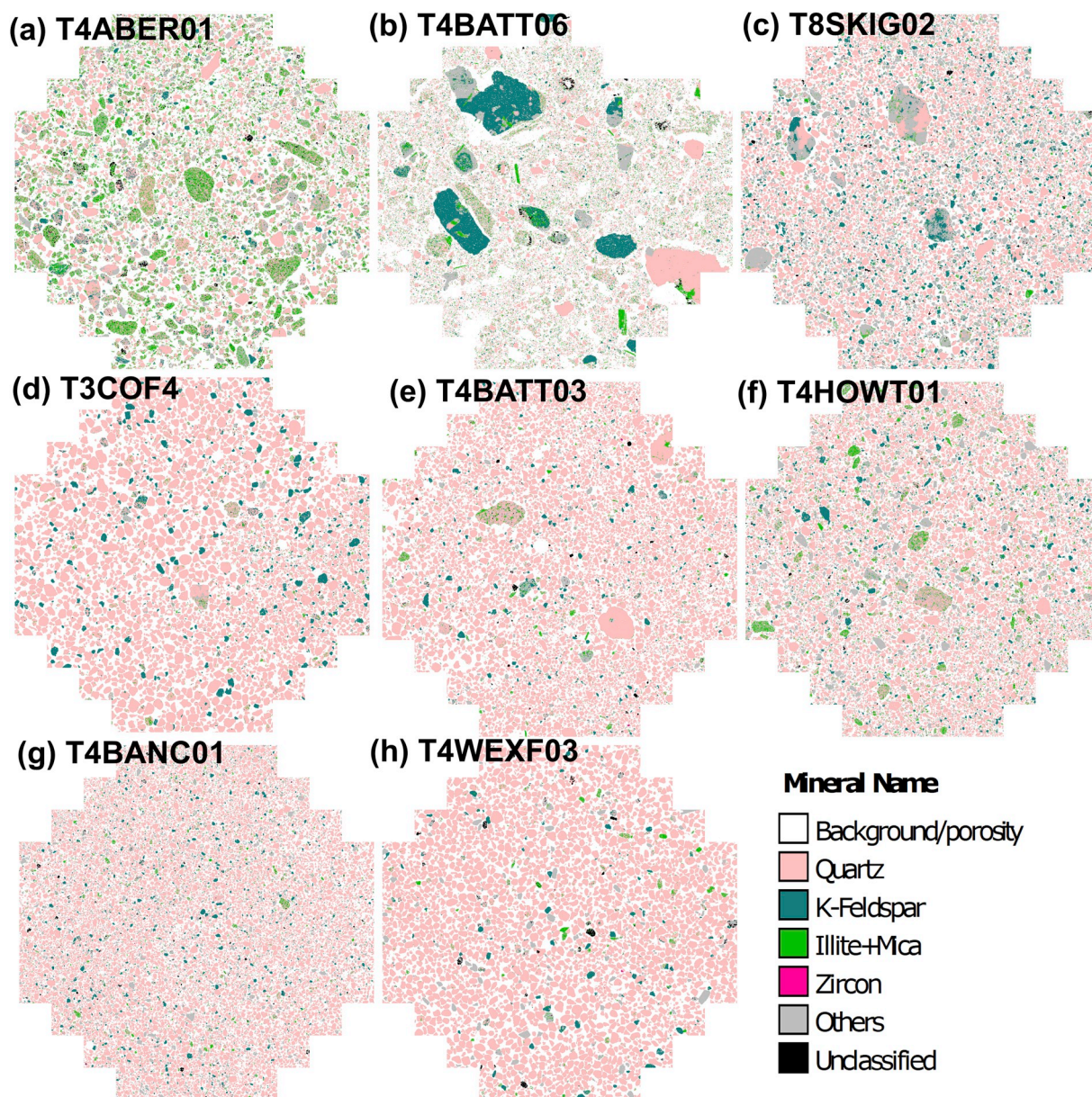
Fig. 6. QEMSCAN® images of 16.5 by 16.5 mm of bulk sediment from a sub-sample of the samples mounted as thin sections made from loose sediment samples poured into a mould and impregnated (i.e. not true *in situ* representations). The samples are ordered according to the RSD of the beta dose-rate heterogeneity for each sample, from lowest (T4ABER01, RSD = 0.2) to highest (T4WEXF03, RSD = 1.1).

should be used. The trend between the RSD of the beta-dose heterogeneity and the beta dose-rate (Fig. 3c) offers a new opportunity to infer the RSD of the beta-dose heterogeneity for each sample using just the beta dose-rate, instead of performing autoradiography on every sample. For this suite of large sedimentary samples, we observed a minimum OD of 20% arising from the effects of beta-dose heterogeneity (Fig. 3e). OD of 20% should be added (in quadrature) to the intrinsic OD to determine σ_b for the MAM to calculate accurate OSL ages and prevent underestimation of the burial age. This approach was applied for single-grain OSL dating of quartz across the former British-Irish Ice Sheet and provided ages in excellent agreement with independent age control (e.g. Smedley et al., 2017a,b; Chiverrell et al., 2018; Small et al., 2017).

Appendix A. Supplementary data

Supplementary data to this article can be found online at https://doi.org/10.1016/j.quageo.2020.101052.

References

Adamiec, G., Heer, A.J., Bluszcz, A., 2012. Statistics of count numbers from a photomultiplier tube and its implications for error estimation. Radiat. Meas. 47, 746–751.

Arnold, L.J., Roberts, R.G., 2009. Stochastic modelling of multi-grain equivalent dose (De) distributions: implications for OSL dating of sediment mixtures. Quat. Geochronol. 4, 204–230.

Bluszcz, A., Adamiec, G., Heer, A.J., 2015. Estimation of equivalent dose and its uncertainty in the OSL SAR protocol when count numbers do not follow a Poisson distribution. Radiat. Meas. 81, 46–54.

Bøtter-Jensen, L., Andersen, C.E., Duller, G.A.T., Murray, A.S., 2003. Developments in radiation, stimulation and observation facilities in luminescence measurements. Radiat. Meas. 37, 535–541.

Chiverrell, R.C., Smedley, R.K., Small, D., Ballantyne, C., Burke, M., Callard, L., Clark, C. D., Duller, G.A.T., Evans, E., Fabel, D., Landeghem, K.V., Livingstone, S.J., O Cofaigh, C., Roberts, D., Saher, M., Scourse, J., Thomas, G.S.P., Wilson, P., 2018. Ice margin oscillations during deglaciation of the northern Irish sea basin. J. Quat. Sci. 33, 739–762.

Cunningham, A., DeVries, D.J., Schaart, D.R., 2012. Experimental and computational simulation of beta-dose heterogeneity in sediment. Radiat. Meas. 47, 1060–1067.

Duller, G.A.T., 2003. Distinguishing quartz and feldspar in single grain luminescence measurements. Radiat. Meas. 37, 161–165.

Duller, G.A.T., 2008. Single-grain optical dating of Quaternary sediments: why aliquot size matters in luminescence dating. Boreas 37, 589–612.

Galbraith, R.F., Laslett, G.M., 1993. Statistical models for mixed fission track ages. Int. J. Radiat. Appl. Instrum. Nucl. Tracks Radiat. Meas. 21, 459–470.

Galbraith, R.F., Roberts, R.G., Laslett, G.M., Yoshida, H., Olley, J.M., 1999. Optical dating of single and multiple grains of quartz from Jinmium rock shelter, northern Austrailia: part I, experimental design and statistical models. Archaeometry 41, 339–364.

Geach, M.R., Thomsen, K.J., Buylaert, J.-P., Murray, A.S., Mather, A.E., Telfer, M.W., Stokes, M., 2015. Single-grain and multi-grain OSL dating of river terrace sediments in the Tabernas Basin, SE Spain. Quat. Geochronol. 30, 213–218.

Guérin, G., Mercier, N., Adamiec, G., 2011. Dose-rate conversion factors: update. Ancient TL 29, 5–8.

Guérin, G., Mercier, N., Nathan, R., Adamiec, G., Lefrais, Y., 2012. On the use of the infinite matrix assumption and associated concepts: a critical review. Radiat. Meas. 47 (9), 778–785.

Guérin, G., Jain, M., Thomsen, K.J., Murray, A.S., Mercier, N., 2015. Modelling dose rate to single grains of quartz in well-sorted sand samples: the dispersion arising from the presence of potassium feldspars and implications for single grain OSL dating. Quat. Geochronol. 27, 52–65.

Guérin, G., Christophe, C., Philippe, A., Murray, A.S., Thomsen, K.J., Tribolo, C., Urbanova, P., Jain, M., Guibert, P., Mercier, N., Kreutzer, S., Lahaye, C., 2017. Absorbed dose, equivalent dose, measured dose rates, and implications for OSL age estimates: introducing the Average Dose Model. Quat. Geochronol. 41, 163–173.

Haberlah, D., Williams, M.A.J., Halverson, G., McTainsh, G.H., Hill, S.M., Hrstka, T., Jaime, P., Butcher, A.R., Glasby, P., 2010. Loess and floods: high-resolution multi-proxy data of last glacial maximum (LGM) slackwater deposition in the flinders ranges, semi-arid south Austrailia. Quat. Sci. Rev. 29, 19–20.

Jacobs, Z., Duller, G.A.T., Wintle, A.G., 2006. Interpretation of single-grain De distributions and calculation of De. Radiat. Meas. 41, 264–277.

Jacobs, Z., Li, B., Jankowski, N., Soressi, M., 2015. Testing of a single grain OSL chronology across the middle to upper palaeolithic transition at Les Cottes (France). J. Archaeol. Sci. 54, 110–122.

Jankowski, N.R., Jacobs, Z., 2018. Beta dose variability and its spatial contextualisation in samples used for optical dating: an empirical approach to examining beta microdosimetry. Quat. Geochronol. 44, 23–37.

Kalchgruber, R., Fuchs, M., Murray, A.S., Wagner, G.A., 2003. Evaluating dose-rate distributions in natural sediments using α-$_{Al2O3}$: C grains. Radiat. Meas. 37, 293–297.

Martin, L., Incerti, S., Mercier, N., 2015. DosiVox: Implementing Geant 4-based software for dosimetry simulations relevant to luminescence and ESR dating techniques. Ancient TL 33, 1–10.

Mayya, Y.S., Morthekai, P., Murari, M.K., Singhvi, A.K., 2006. Towards quantifying beta microdosimetric effects in single-grain quartz dose distribution. Radiat. Meas. 41, 1032–1039.

Meyer, M.C., Austin, P., Tropper, P., 2013. Quatitative evaluation of mineral grains using automated SEM-EDS analysis and its application potential in optically stimulated luminescence dating. Radiat. Meas. 58, 1–11.

Murray, A.S., Wintle, A.G., 2000. Luminescence dating of quartz using an improved single-aliquot regenerative-dose protocol. Radiat. Meas. 32, 57–73.

Nathan, R.P., Thomas, P.J., Jain, M., Murray, A.S., Rhodes, E.J., 2003. Environmental dose rate heterogeneity of beta radiation and its implications for luminescence dating: Monte Carlo modelling and experimental validation. Radiat. Meas. 37, 305–313.

Olley, J.M., Caitcheon, G.G., Roberts, R.G., 1999. The origin of dose distributions in fluvial sediments, and the prospect of dating single grains from fluvial deposits using optically stimulated luminescence. Radiat. Meas. 30, 207–217.

Prescott, J.R., Hutton, J.T., 1994. Cosmic-ray contributions to dose-rates for luminescence and Esr dating - large depths and long-term time variations. Radiat. Meas. 23, 497–500.

Rufer, D., Preusser, F., 2009. Potential of autoradiography to detect spatially resolved radiation patterns in the context of trapped charge dating. Geochronometria 34, 1–13.

Small, D., Clark, C., Bateman, M.B., Chiverrell, R.C., Smedley, R.K., Duller, G.A.T., Ely, J. C., Fabel, D., Medialdea, A., Moreton, S.G., 2017. Devising quality assurance procedures for assessment of legacy geochronological data relating to deglaciation of the last British-Irish Ice Sheet. Earth Sci. Rev. 164, 232–250.

Smedley, R.K., Chiverrell, R.C., Burke, M.J., Duller, G.A.T., Thomas, G.S.P., Clarke, C., Scourse, J., 2017a. Internal dynamics condition millennial-scale oscillations of a retreating ice stream margin. Geology 45, 787–790.

Smedley, R.K., Scourse, J.D., Small, D., Hiemstra, J.F., Duller, G.A.T., Bateman, M.D., Burke, M.J., Chiverrell, R.C., Clark, C.D., Davies, S.M., Fabel, D., Gheorghiu, D.M., McCarroll, D., Medialdea, A., Xu, S., 2017b. New age constraints for the limit of the British-Irish ice sheet on the Isles of scilly. J. Quat. Sci. 32, 48–62.

Thomsen, K.J., Murray, A.S., Bøtter-Jensen, L., 2005. Sources of variability in OSL dose measurements using single grains of quartz. Radiat. Meas. 39, 47–61.

Thomsen, K.J., Murray, A.S., Bøtter-Jensen, L., Kinahan, J., 2007. Determination of burial dose in incompletely bleached fluvial samples using single grains of quartz. Radiat. Meas. 42, 370–379.

Thomsen, K.J., Murray, A.S., Buylaert, J.P., Jain, M., Hansen, J.H., Aubry, T., 2016. Testing single-grain quartz OSL methods using sediment samples with independent age control from the Bordes-Fitte rockshelter (Roches d'Abilly site, Central France). Quat. Geochronol. 31, 77–96.

Thrasher, I.M., Mauz, B., Chiverrell, R.C., Lang, A., Thomas, G.S.P., 2009. Testing an approach to OSL dating of Late Devensian glaciofluvial sediments of the British Isles. J. Quat. Sci. 24, 785–801.

Trauerstein, M., Lowick, S., Preusser, F., Veit, H., 2017. Testing the suitability of dim sedimentary quartz from northern Switzerland for OSL burial dose estimation. Geochronometria 44, 66–76.